CHEMISTRY
AN ASIAN JOURNAL

DOI: 10.1002/asia.200700323

Stability of Alkali Metal Halide Polymorphs as a Function of Pressure

Željko P. Čančarević, J. Christian Schön,* and Martin Jansen*[a]

Abstract: We investigated the regions of thermodynamic stability of possible modifications of the alkali metal halides as a function of pressure and type of alkali metal and halogen. Both Hartree–Fock and density functional calculations (for six different functionals) were performed. The results are in good agreement with experiment, and the trends in the computed quantities such as transition pressures and lattice parameters as a function of the ab initio method are similar to those found in earlier studies of the alkali metal sulfides. We predict that in most of these systems the so-called 5–5 modification should be metastable at standard pressure and be thermodynamically stable at slightly negative pressures. The sizes of the pressure ranges over which the various modifications are stable showed characteristic trends as a function of the type of the constituent elements, thus generalizing the traditional pressure–homologue rule for transition pressures and stable phases in ionic solids.

Keywords: ab initio calculations · alkali metals · halides · structural transitions · structure prediction

Introduction

In recent years, experiments at very high pressures exceeding 10 GPa have become more common,[1,2] thus leading to an enormous increase in the number of new high-pressure phases discovered in various chemical systems. However, in spite of highly improved experimental techniques, the measurement of the structures of these compounds in situ are still far from trivial, and in many instances the only reliable information obtained is the cell constants of the modification under investigation. Thus, it would be very helpful for the identification of newly generated phases if one could supplement the experimental results by theoretical investigations on the same system. However, not just the high-pressure region has received increased attention. Even more fascinating is the observation that new experimental techniques, such as the growth of crystalline compounds in an amorphous matrix of the same atomic composition, which had been deposited at very low temperatures (liquid-nitrogen or liquid-helium temperatures) by using atom beams,[3–6] lead to metastable compounds that would be thermodynamically stable at negative pressures.

This poses a new challenge to the theoretician, as one can no longer expect that all relevant structure candidates at high positive and negative pressures also show local minima of the potential energy, that is, of the enthalpy at zero pressure. Instead, it is necessary to study the enthalpy surface at many different pressures to determine as many candidates as possible for such extreme conditions. The procedure is completely analogous to structure prediction for solids at low (zero) pressure by the determination of local minima of the potential energy of the system.[7–11] In earlier works,[12–15] we have shown for several binary nitrides, sulfides, and oxides how one can identify such structures and predict their transition pressures.

Clearly, it would be of interest to know to what extent these landscapes differ within a family of chemically related systems. There exists the well-known pressure homologue rule,[16] according to which the pressure-induced transitions between two modifications within a family of compounds take place at decreasing pressure for increasing size of cation for a fixed choice of anion. Two questions should be addressed: First, can we formulate an analogous rule for families of compounds whereby the cation is kept fixed instead of the anion? Second, what happens in the opposite region of the pressure line, that is, at what effective negative pressure do we find a new compound with lower coordination numbers, and does this transition pressure also obey some analogous pressure–homologue rule? Up to now, our investigations point to the fact that one should view the tra-

[a] Dr. Ž. P. Čančarević, Prof. Dr. J. C. Schön, Prof. Dr. M. Jansen
Max-Planck-Institut für Festkörperforschung
Heisenbergstr. 1, 70569 Stuttgart (Germany)
Fax: (+49) 711-689-1502
E-mail: c.schoen@fkf.mpg.de
m.jansen@fkf.mpg.de

Supporting information for this article is available on the WWW under http://www.chemasianj.org or from the author.

ditional pressure–homologue rule as "one half" of a more general rule, according to which the size of pressure regions in which a modification is stable changes as a function of cation size in families of compounds.[13] Notably, the choice of ab initio method (Hartree–Fock approximation, density functional) had a strong influence on the absolute values of the transition pressures between the various modifications. Nevertheless, if one considers the results of a given family of compounds for only one ab initio method, the generalized pressure–homologue rule is approximately fulfilled.

In this work, we investigate the possible modifications of the alkali metal halides as a function of pressure, as there exists a large number of experimental observations and theoretical calculations,[1] which can be employed to validate the computations presented herein. Since the early studies by Madelung,[17] Ewald,[18] and Born and Huang,[19] alkali metal halides have been the subject of a large number of theoretical investigations. The simple Born-type semiempirical formula for the interatomic potential energy (a Coulomb or "Madelung" long-range term and a short-range repulsive term) used in the early studies was supplemented in the 1960s by dipole,[20] quadrupole,[21] and/or breathing-shell[22] terms. In the 1970s, a more fundamental approach, still partly empirical and based on electron–gas theory,[23–25] was applied systematically to the alkali metal halides and other compounds. The earliest quantum-mechanical work by Löwdin[26] involved numerous approximations in the theory. In the 1980s and especially in the 1990s, the implementation of reasonably reliable fully ab initio schemes allowed the nonempirical evaluation of the structural properties of ionic systems with reference to both the density functional (DFT)[27–31] and Hartree–Fock[32,33] (HF) Hamiltonians. Many of these pioneering ab initio calculations were plagued by problems of numerical accuracy, basis-set limitations, or simply the reliability of computer programs. In the late 1990s, considerable progress was made in the direction of standardization, generalization, and improvement of the numerical accuracy of the algorithms of many computational schemes. During this time, systematic investigations were performed,[34] which show the limits and merits of the adopted Hamiltonians, schemes of the solutions of the Schrödinger equation and choices of basis sets.

Common to all the investigations mentioned above is that only two possible AB structure types (B1 (NaCl) and B2 (CsCl)) were investigated.[2] Furthermore, there is a lack of systematic comparison of different Hamiltonians, especially with different correlation-exchange combinations. Thus, in this work, we extend these earlier investigations in three directions: 1) we consider the whole pressure range from moderate negative pressures to high positive pressures, 2) we perform global optimizations on the energy/enthalpy landscapes of all 20 alkali metal halides to identify additional potential structure candidates, and 3) for a small group of the most important modifications at moderate negative and positive pressures we calculate the transition pressures by using seven different ab initio methods (Hartree–Fock and six density functionals).

[1] Typically, energy-related properties such as cell geometry, atomic fractional coordinates, transition pressures, or elastic properties were computed in these studies.

[2] In most of cases only the B1 (NaCl) structure was considered.

Methods

General Approach and Modeling of the Empirical Energy Landscape

Our general approach to the determination of structure candidates is given in detail elsewhere.[7] Here we just summarize the procedure: The structure candidates that should be capable of existence, at least at low temperatures, correspond to local minima of the enthalpy hypersurface ($H = E_{pot} + pV$) of the chemical system under investigation. Finding these candidates requires the use of a global optimization method as well as local optimization procedures, because we permit free variation of atom positions, cell parameters, ionic charges, and composition during the exploration of the global landscape. To determine the most important local minima of the energy/enthalpy landscapes of the systems under investigation, many thousands of global optimization runs have to be performed. As global optimization methods, in general, involve many millions of energy evaluations for atomic configurations, one cannot perform the energy calculation with ab initio methods or elaborate but computationally intensive empirical potentials for a study of this size. Therefore, we modeled the systems as spherical ions that interact by a simple empirical two-body interaction potential, $V_{ij}(r_{ij})$, consisting of a Coulomb and a Lennard–Jones term that depend only on the atom–atom distance r_{ij}, to allow fast calculations of the energy, $E_{pot} = \Sigma_{i<j} V_{ij}(r_{ij})$, of a given configuration [Eq. (1)]:

$$V_{ij}(r_{ij}) = \frac{q_i q_j}{r_{ij}} \exp(-\mu r_{ij}) + \varepsilon_{ij}\left[\left(\frac{\sigma_{ij}}{r_{ij}}\right)^{12} - \left(\frac{\sigma_{ij}}{r_{ij}}\right)^{6}\right] \quad (1)$$

The parameters that make up the empirical potential are the sum of the ionic radii multiplied by a scaling factor r_s, $\sigma_{ij} = r_s(r_{ion}(i) + r_{ion}(j))$, the standard Lennard–Jones parameters ε_{ij}, and the convergence parameter μ. To compute the electrostatic energy during the global optimization stage, an Ewald summation is often employed, as proposed by de Leeuw et al.,[35] instead of the convergence parameter μ. However, at this stage, we are mostly interested in calculational speed and in the possible structures, and not so much in their precise energies. The actual energies of the structures will be computed later by employing ab initio methods during local optimization. Similarly, we varied the values of $r_s \approx 1$ and ε_{ij} (=0.3–0.5) between optimization runs to judge the robustness of the structure candidates.[36] The ionic radii employed during the optimization were: $r_{ion}(Li^+) = 0.78$, $r_{ion}(Na^+) = 0.98$, $r_{ion}(K^+) = 1.33$, $r_{ion}(Rb^+) = 1.49$, $r_{ion}(Cs^+) = 1.65$, $r_{ion}(F^-) = 1.33$, $r_{ion}(Cl^-) = 1.81$, $r_{ion}(Br^-) = 1.96$, and $r_{ion}(I^-) = 2.20$ Å.

As we are interested in crystalline compounds, we introduced periodic boundary conditions and employed up to

four formula units of the respective compounds per simulation cell. While our general moveclass (=set of allowed exploration moves) also involves changes of composition and charges, in this work, we kept the composition (M/X=1:1) and the charges ($q_{cation}=+1$, $q_{anion}=-1$) fixed.

Global and Local Optimization Procedures

The global optimizations were performed by employing the stochastic simulated annealing algorithm,[37,38] which is based on random walks on the energy landscapes. Each step from configuration x_i to a neighbor x_{i+1} was accepted according to the Metropolis criterion,[39] with a temperature schedule $T_n=T_0\gamma^n$ ($\gamma=0.995$). Each run consisted of 1000 temperature changes with 800 steps per temperature. The moveclass consisted of atom movement, atom exchange, and random variations of the cell parameters while the ionic charges were kept fixed. For each pressure, 90 simulated annealing runs were performed.

The calculations were repeated for a number of pressures ($p=0$, -16, -160, 0.16, 1.6, 16, 160, 1600 GPa). The reason for this choice of pressures is that, owing to the functional form of the core-repulsion potential ($V\propto r^{-12}$), we expect the changes in the landscape between subsequent "high" values of pressure to occur at considerably larger absolute-pressure differences than at "low" pressure values. Owing to the rather widely spaced set of pressure values, calculation of the transition pressure is not possible at this stage, but we can expect to gain a good overview of the structure candidates as a function of pressure. The possible phase transitions between these candidates will then be determined at the ab initio stage of the procedure.

As the structure candidates were found by using a simple empirical potential as a cost function, we are faced with two problems. First, the structure candidates will not usually exhibit any obvious symmetries (they are given in space group $P1$, due to the unrestricted optimization procedure), and it is often difficult to decide just by visual inspection whether two configurations correspond to the same structure. To deal with this issue, we used the algorithms SFND,[40] RGS,[41] and CMPZ,[42] as implemented in the program KPLOT,[43] to identify the symmetries and the space groups of the optimal configurations, followed by an idealization of the structure according to the space group and an elimination of duplicate structures. Furthermore, because we had to use empirical parameters for the ionic radii and Lennard–Jones interaction strengths, the nearest-neighbor distances among the atoms are not necessarily in agreement with those one would observe in experiment. Both the size of the unit cell and the relative atom positions might differ somewhat from the experimental values, thus making a comparison between predicted and subsequently synthesized compounds difficult.

Thus, when we rank the candidates by energy by employing the ab initio program CRYSTAL2003,[44] we need to perform a local optimization of the cell parameters and atom positions. To deal with the problem in an efficient way, we developed the heuristic algorithm HARTREE,[45,13] which performs the local optimization in an automated manner. For each distinct structure candidate, after symmetry identification and idealization, we refined the structure by varying the cell parameters and the atom positions until a minimum in the energy was found. During these optimizations, we usually restricted the variation of these parameters such that the space-group symmetry that had been determined during the idealization stage was preserved. To gain an estimate of the validity of the ab initio calculations, we performed both Hartree–Fock and DFT (six different functionals: B3LYP, BECKE-LYP, BECKE-PWGGA, LDA-LYP, LDA-PWGGA, LDA-VBH) calculations for all structures and systems.

Besides the optimized cell parameters, these calculations yield the bulk modulus B_0 by fitting the calculated data points to the Murnaghan equation [Eq. (2)]:[46]

$$E(V)=\frac{VB_0}{B_0'}\left[\frac{(V_0/V)^{B_0'}}{B_0'-1}+1\right]-C \qquad (2)$$

in which the four fit parameters B_0 and B_0' are the bulk modulus and its derivative, V_0 is the equilibrium volume, and C is the adjustment of the zero of the energy scale. By calculating the enthalpies $H_i=E_i(V)+pV=E_i(V)-(\partial E/\partial V)V$ for the various structure candidates i, one can determine the transition pressures between different modifications i and j by setting the enthalpies to be equal ($H_i=H_j$).[3]

Basis-Set Optimization

The choice of a basis set is a crucial step of the calculation, as we have to balance two conflicting issues, accuracy and computational cost,[4] while taking the minimum basis-set requirements into account.[5]

To determine which combination of basis sets is optimal, a number of basis sets were tested for the present alkali metal halide calculations. Some of the basis sets were all-electron basis sets[47] (AEBS)[6] or Hay and Wadt (HW) effective-core-pseudopotential (ECP) basis sets (PPBS),[47][7] and some were "Stuttgart/Cologne-type" pseudopotential basis

[3] It follows from $H_i=H_j$ that the transition pressure p_c is given as the negative slope of the common tangent of $E_i(V)$ and $E_j(V)$.

[4] As our study required the comparison of energies for very different crystal configurations and structures, rather high accuracy was necessary. The self-consistent-field (SCF) convergence criterion is that the change in the total energy between two iterations amounted to less than 10^{-8} hartree.

[5] One commonly chosen solution to this problem (especially for heavy atoms such as Rb and Cs) is to attempt to summarize the effects of the core electrons in an effective averaged pseudopotential, which decreases the number of coefficients in the wavefunction (that still needs to be optimized, of course). Notably, pseudopotentials do not yield the true energy, and thus a direct comparison with energies based on all-electron-basis-set (AEBS) calculations is not possible—only energy differences are meaningful in such a case.

[6] Li (6-11G), Na (8-511G*), K (86-511G*), F (7-311G), Cl (86-311G).

[7] Br: [HAYWSC]-31, small-core pseudopotential; I: [HAYWLC]-31 large-core pseudopotential.

Table 1. Summary of basis-set optimizations for the AX system (A = Li, Na, K, Rb, Cs; X = F, Cl, Br, I).[a]

System	Element	Basis set	Ref.	Shell no.	Shell type	Exponent	System	Element	Basis set	Ref.	Shell no.	Shell type	Exponent
LiF	Li	6-11G	[47]	2	sp	0.5147	KBr	K	865-11Gd	[47]	4	sp	0.3949
				2	sp	2.0376					4	sp	0.2170
	F	7-311G	[47]	2	sp	0.4379					4	d	0.3774
				2	sp	0.1709		Br	HAYWLC-31	[47]	4	sp	0.0989
LiCl	Li	6-11G	[47]	2	sp	0.5315	KI	K	865-11Gd	[47]	4	sp	0.3963
				2	sp	0.2088					4	sp	0.2169
	Cl	86-311G	[47]	3	sp	0.3117					4	d	0.4750
				3	sp	0.1172		I	HAYWLC-31	[47]	5	sp	0.0885
LiBr	Li	6-11G	[47]	2	sp	0.5280	RbF	Rb	ECP25MWB	[48]	5	p	0.3273
				2	sp	0.1745					5	p	0.1329
	Br	HAYWLC-31	[47]	4	sp	0.0999					5	d	0.3592
LiI	Li	6-11G	[47]	2	sp	0.5258		F	7-311G	[47]	2	sp	0.4363
				2	sp	0.1585					2	sp	0.1483
	I	HAYWLC-31	[47]	5	sp	0.0885	RbCl	Rb	ECP25MWB	[48]	5	p	0.3262
NaF	Na	85-11G*	[47]	3	sp	0.5452					5	p	0.1340
				3	sp	0.2176					5	d	0.2967
				3	*	0.6792		Cl	86-311G	[47]	3	sp	0.3154
	F	7-311G	[47]	2	sp	0.4303					3	sp	0.1156
				2	sp	0.1533	RbBr	Rb	ECP25MWB	[48]	5	p	0.3248
NaCl	Na	85-11G*	[47]	3	sp	0.5353					5	p	0.1328
				3	sp	0.1803					5	d	0.3032
				3	*	0.3501		Br	HAYWLC-31	[47]	4	sp	0.0975
	Cl	86-311G	[47]	3	sp	0.3144	RbI	Rb	ECP25MWB	[48]	5	p	0.3255
				3	sp	0.1217					5	p	0.1347
NaBr	Na	85-11G*	[47]	3	sp	0.5390					5	d	0.3147
				3	sp	0.2021		I	HAYWLC-31	[47]	5	sp	0.0880
				3	*	0.2675	CsF	Cs	ECP46MWB	[48]	6	p	0.2823
	Br	HAYWLC-31	[47]	4	sp	0.1006					6	p	0.1124
NaI	Na	85-11G*	[47]	3	sp	0.5397					6	d	0.2678
				3	sp	0.2097		F	7-311G	[47]	2	sp	0.4378
				3	d	0.2301					2	sp	0.1469
	I	HAYWLC-31	[47]	5	sp	0.0889	CsCl	Cs	ECP46MWB	[48]	6	p	0.2817
KF	K	865-11Gd	[47]	4	sp	0.3902					6	p	0.1158
				4	sp	0.2207					6	d	0.2467
				4	d	0.5656		Cl	86-311G	[47]	3	sp	0.3168
	F	7-311G	[47]	2	sp	0.4325					3	sp	0.1139
				2	sp	0.1476	CsBr	Cs	ECP46MWB	[48]	6	p	0.2814
KCl	K	865-11Gd	[47]	4	sp	0.3941					6	p	0.1161
				4	sp	0.2212					6	d	0.2527
				4	d	0.4218		Br	HAYWLC-31	[47]	4	sp	0.0966
	Cl	86-311G	[47]	3	sp	0.3170	CsI	Cs	ECP46MWB	[48]	6	p	0.2810
				3	sp	0.1178					6	p	0.1162
											6	d	0.2538
								I	HAYWLC-31	[47]	5	sp	0.0873

[a] The outermost-shell exponents were optimized. According to standard terminology and notation connected with Gaussian basis sets, an asterisk is added to the basis-set symbol to indicate the presence of polarization functions. In the table, polarization functions are represented as d orbitals. Only the hydrogen atom has p orbitals as polarization functions; all other elements have d orbitals.

sets[48] (PPBS),[8] as in the case of Rb (ECP28MWB) and Cs (ECP46MWB). The outermost shell exponents were optimized through energy minimization of the crystal energy for all of the system explored. The reoptimized basis sets are given in Table 1.

Results

Results of the Global Search

Apart from structures with space group $P1$ or $P\bar{1}$, about 270 different structure types were observed to constitute local minima on the various enthalpy landscapes. Of these, 35 candidate structures could be identified with experimentally known structure types by using the automated structure comparison script FILTER,[9] which employs the CMPZ[42] al-

[8] According to library keywords of pseudopotentials of the Stuttgart/Cologne group,[48] these are of the form ECP*n*XY; *n* is the number of core electrons that are replaced by the pseudopotential, X denotes the reference system used for generating the pseudopotential (X = M: neutral atom), and Y stands for the theoretical level of the reference data (Y = WB: quasi-relativistic).

[9] The full heuristic algorithm[45] contains the following steps: idealization (LOAD script), sorting (FILTER script), and preliminary ranking of the structure candidates found by global optimization, followed by a local optimization (HARTREE script).

gorithm. Lists of the new structure types for all 20 alkali metal halides are given in the Supporting Information (see Tables 1.8, 1.17, 1.26, 1.35, 1.44, 1.53, 1.62, 1.71, 1.80, 1.89, 1.98, 1.107, 1.116, 1.125, 1.134, 1.143, 1.152, 1.161, 1.170, 1.179 there).[10] An overview of the different structure candidates found in the 20 alkali metal halide systems as a function of pressure is given in Figure 1. For each pressure range and alkali metal halide, those among the 35 known structure types mentioned above that were observed during the optimizations are represented by a symbol. The number of times a given type was detected is indicated by the number inside the symbol. Furthermore, the number of additional structure types (with space groups other than $P1$ or $P\bar{1}$) that were found at this pressure is also given in Figure 1.

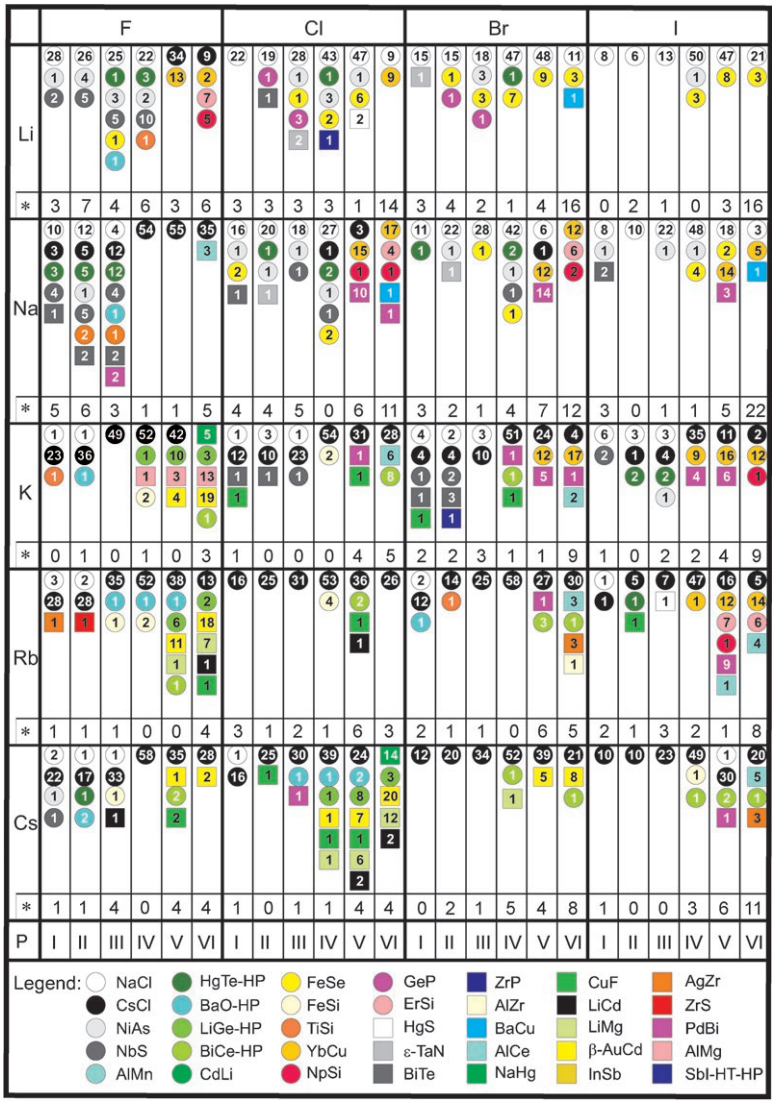

Figure 1. Distribution of the structure candidates (belonging to structure types already known) for different pressures. Only results for positive pressures are shown. The roman numerals I–VI indicate the pressures 0, 0.16, 1.6, 16, 160, and 1600 GPa, respectively. Structures with space groups $P1$ and $P\bar{1}$ are not listed. About 235 additional different structure types were observed to constitute minima on various enthalpy landscapes (not counting structures with space group $P1$ or $P\bar{1}$). In the rows indicated by an asterisk, the number of additional structure types for the given pressure and alkali metal halide is given.

Notably, the rock-salt, CsCl, and NiAs structure type were found for all of the alkali metal halides. Figure 1 shows that for each pressure, between one and three quarters of the optimization runs resulted in structures with space groups other than $P1$ or $P\bar{1}$, with a clear peak at the high end of the intermediary pressure range. If we discard the duplicates, then the fraction of runs resulting in different structures with higher symmetry than $P\bar{1}$ or $P1$ for a particular halide at a given pressure ranged from 20 to 42%. Furthermore, the number of different structure types summed over all pressures for a given system ranged from 16 for KF to 42 for NaCl. Generally, the structural diversity as indicated by the number of distinct local minima found on the various enthalpy landscapes appears to be greater for cations of smaller size.

Our experience has shown for landscapes of families of related chemical systems[36,49,14,13] that many of the structure types that were not explicitly found in a given chemical system during the global optimization nevertheless correspond to local minima on these landscapes. These minima are typically not very deep and have only a small attraction basin, and thus are less likely to be observed during the still-limited number of global optimization runs. The fact that many minima were only found once per system and pressure clearly shows that we have not yet reached the saturation level of the global optimization procedure, that is, a statistically stable distribution of occurrence of local minima during the stochastic optimization. For our purposes, this is not a critical problem. In fact, it would not be an effective use of computational resources to actually reach saturation, as our goal is to identify as many different structure candidates in a

[10] Notably, these structures are named according to the chemical system in which they were first registered. As the systems were investigated starting with the lithium halides and ending with the cesium halides, the names are heavily weighted towards the first group of halides.

family of chemical systems as possible for the least computational effort.

As structures are typically present as local minima not only on one but on most of these landscapes, it has therefore proven to be very useful to supplement the set of structure candidates found during the global optimization by additional candidates observed in related chemical systems before starting the local optimizations. We then tested whether these additional structures also constitute local minima on the empirical energy landscape, or if they represent structures that are energetically low stable local minima at the ab initio level. Thus, we added several well-known candidates that had been found on the enthalpy landscapes of the various AB systems for the local optimization step at the ab initio level. In particular, we included a few of the most prominent low-density AB structure types (wurtzite, sphalerite, β-BeO, 5–5[36]) that had been observed in an earlier investigation of the landscape of NaCl[36] with a different annealing schedule, during a global exploration of the landscape of LiF at the ab initio level,[50] and during a study of the alkaline earth oxides[14] with the threshold algorithm.[51] In the present study, the optimizations at negative pressures did not result in finding many periodic low-density structure candidates that exhibit a low enthalpy; thus, we did not include the statistics for negative pressures in the overview in Figure 1. Generally, it has already been found in other chemical systems that the landscapes for effective negative pressures are relatively difficult to explore with standard global optimization methods, because at negative pressures well-ordered, low-density crystalline structures always compete with a plethora of slab-, rod-, or clusterlike structures that often exhibit very low enthalpies.[14]

Overview of Results of Local Optimizations

In earlier work,[13] we compared several ab initio techniques with regard to their performance. On the basis of these results, we decided to apply the same scheme to the local refinement optimizations of the alkali metal halides, that is, the calculations ranged from Hartree–Fock (HF) over hybrid B3LYP and semilocal gradient-dependent functionals (BECKE-LYP and BECKE-PWGGA) to local functionals (LDA-VBH). Furthermore, we employed two rather uncommon combinations of gradient-dependent and local functionals (LDA-LYP and LDA-PWGGA).

Table 2 gives an overview of the lattice parameters a and the bulk modulus B_0 at zero pressure and zero temperature for the rock-salt modifications of all 20 alkali metal halides calculated by using the seven ab initio methods. The analogous results for the other modifications are given in the Sup-

Table 2. Calculated and experimental lattice parameters and bulk moduli for the rock-salt B1 structure type in the AX system (A = Li, Na, K, Rb, Cs; X = F, Cl, Br, I).

	Method	F		Cl		Br		I	
		a [Å]	B_0 [GPa]	a [Å]	B_0 [GPa]	a [Å]	B_0 [GPa]	a [Å]	B_0 [GPa]
Li	HF	4.01464	70.453	5.29590	27.122	5.74382	20.087	6.32938	14.121
	DFT-B3LYP	4.04415	67.714	5.23086	28.941	5.64171	22.726	6.16553	16.698
	BECKE-LYP	4.10114	61.658	5.28546	26.894	5.68906	21.397	6.21137	15.702
	BECKE-PWGGA	4.10104	58.976	5.24657	27.169	5.64572	21.721	6.12510	17.108
	LDA-LYP	3.84711	97.176	4.93813	43.787	5.33009	34.758	5.79716	27.281
	LDA-PWGGA	3.82782	97.346	4.87538	45.676	5.25887	36.856	5.69517	30.563
	LDA-VBH	3.91167	85.378	5.02455	38.161	5.41435	30.387	5.88048	24.030
	Theory	3.85–4.05	70.5–99.6	5.03–5.28	30.0–40.8	5.44–5.73	21.4–31.0	5.93–6.32	15.4–22.0
	Ref.	[52, 30, 34, 53]	[52, 30, 34, 53]	[52, 30, 34, 53]	[52, 30, 34, 53]	[30, 53]	[30, 53]	[30, 53]	[30, 53]
	Experiment	4.03–4.05	64.9–76.9	5.13–5.17	31.8–36.9	5.49–5.51	25.7–30.1	6.00–6.06	18.8
	Ref.	[54–60]	[61]	[62, 63, 57, 64]	[61]	[62, 63, 57]	[61]	[62, 63, 57]	[61]
Na	HF	4.63227	48.992	5.78789	21.779	6.20947	16.115	6.76566	11.539
	DFT-B3LYP	4.66002	46.603	5.72246	23.065	6.10157	18.243	6.60387	13.657
	BECKE-LYP	4.72599	42.179	5.78178	21.260	6.15438	17.207	6.65727	12.752
	BECKE-PWGGA	4.74896	38.075	5.77512	20.102	6.14340	16.393	6.60844	12.980
	LDA-LYP	4.41805	70.772	5.36590	37.276	5.74208	30.128	6.18537	23.844
	LDA-PWGGA	4.41127	67.814	5.31926	37.849	5.68796	30.705	6.10200	25.534
	LDA-VBH	4.50153	58.807	5.47121	31.102	5.84487	25.418	6.28788	20.205
	Theory	4.76–5.03	42.3–69.6	5.52–5.75	22.8–32.3	6.10–6.23	18.6–23.5	6.58–6.65	12.3–14.9
	Ref.	[52, 30, 34, 53]	[52, 30, 34, 53]	[52, 30, 34, 53]	[52, 30, 34, 53]	[30, 53]	[30, 53]	[30, 53]	[30, 53]

Table 2. (Continued)

	Method	F		Cl		Br		I	
		a [Å]	B_0 [GPa]	a [Å]	B_0 [GPa]	a [Å]	B_0 [GPa]	a [Å]	B_0 [GPa]
	Experiment	4.61–4.78	36.9	5.45–5.64	28.6	5.96–6.00	20.8	6.47–6.48	18.7
	Ref.	[65, 55, 66, 67, 57, 68, 59, 69]	[61]	[70, 55, 57, 71, 72, 73, 74, 75, 76, 59, 69]	[61]	[62, 56, 57, 64, 72, 68, 69]	[61]	[62, 57, 77, 78, 79, 69]	[61]
K	HF	5.44898	28.938	6.55424	14.562	6.97708	10.807	7.51817	8.068
	DFT-B3LYP	5.43000	29.214	6.45557	15.503	6.83181	12.054	7.33180	9.036
	BECKE-LYP	5.49566	26.449	6.52271	14.297	6.89192	11.254	7.39857	8.351
	BECKE-PWGGA	5.49333	24.225	6.50440	13.076	6.87623	10.225	7.34426	7.945
	LDA-LYP	5.09640	50.649	6.10070	28.671	6.35593	23.097	6.78625	17.933
	LDA-PWGGA	5.05851	55.479	5.93919	29.607	6.27273	24.061	6.67498	19.598
	LDA-VBH	5.19299	43.401	6.12320	23.338	6.47389	18.795	6.90658	14.660
	Theory	5.40–5.44	30.0–45.0	5.92–6.26	15.1–24.0	6.57–6.59	11.8–17.0	7.01–7.03	9.0–13.8
	Ref.	[52, 30, 34, 53]	[52, 30, 34, 53]	[52, 30, 34, 53]	[52, 30, 34, 53]	[30, 53]	[30, 53]	[30, 53]	[30, 53]
	Experiment	5.34–5.37	30.1	6.27–6.30	23.8	6.58–6.64	17.4	7.05–7.10	15.9
	Ref.	[55, 80, 57]	[61]	[81, 55, 56, 57, 73, 82]	[61]	[83, 62, 56, 57, 82]	[61]	[55, 83, 57, 82]	[61]
Rb	HF	5.82390	23.692	6.91095	12.356	7.33603	9.474	7.85308	7.263
	DFT-B3LYP	5.79642	24.397	6.80442	13.611	7.18075	10.740	7.66250	8.256
	BECKE-LYP	5.86822	23.801	6.87029	12.691	7.23943	10.059	7.72620	7.693
	BECKE-PWGGA	5.85527	21.565	6.84550	11.676	7.21618	9.214	7.67288	7.202
	LDA-LYP	5.43700	49.986	6.34902	25.237	6.68831	20.382	7.10327	16.357
	LDA-PWGGA	5.37745	52.290	6.26508	26.046	6.59284	21.211	6.79660	17.648
	LDA-VBH	5.53921	37.555	6.46283	20.782	6.80835	16.821	7.22775	13.568
	Theory	5.73–6.32	23.4–38.0	6.57–6.79	13.0–22.0	6.88–7.53	10.5–15.1	7.31–7.95	7.4–12.2
	Ref.	[30, 53]	[30, 53]	[30, 53]	[30, 53]	[30, 53]	[30, 53]	[30, 53]	[30, 53]
	Experiment	5.65–6.64	6.58	6.59–6.94	18.6	7.32–7.36	13.9		12.9
	Ref.	[84]	[61]	[62, 85, 56, 86, 82, 87]	[61]	[88, 62, 56, 82]	[61]	[89, 62, 86, 82]	[61]
Cs	HF	6.24891	18.796	7.34131	10.232	7.76084	7.968	8.26923	6.239
	DFT-B3LYP	6.18650	20.015	7.20366	11.421	7.57880	9.138	8.05160	7.137
	BECKE-LYP	6.26121	19.225	7.27006	10.582	7.63875	8.536	8.11725	6.632
	BECKE-PWGGA	6.19030	22.641	7.21117	10.108	7.58141	8.073	8.03063	6.370
	LDA-LYP	5.74763	49.885	6.68854	22.371	7.03331	18.286	7.44034	14.848
	LDA-PWGGA	5.64846	54.933	6.57096	24.256	6.90359	19.873	7.27991	16.620
	LDA-VBH	5.85124	40.557	6.80443	18.490	7.15307	15.172	7.56344	12.369
	Theory	6.02–6.12	23.1	–	–	–	–	–	–
	[Ref.]	[30]	[30]	–	–	–	–	–	–
	Experiment	6.03	–	6.92–7.10	–	7.26	–	7.63	–
	Ref.	[62]	[61]	[90, 91]	–	[91, 82]	–	[91]	–

porting Information. As one would expect from general considerations, the Hartree–Fock calculations produced larger equilibrium volumes and higher transition pressures than the DFT ones, with the experimental values lying somewhere in between. Furthermore, the results of the LDA-type functionals systematically lie below those of the BECKE-type ones, whereas gradient corrections (GGA) do not appear to make much of a difference.

Figure 2 shows which modification was predicted by the various ab initio methods to be thermodynamically stable at standard pressure. No procedure achieves a perfect score; the "best" actually appears to be LDA-VBH and not a mixed functional such as B3LYP, which usually yields quite reasonable quantitative agreement with experiment: Hartree–Fock and Becke-type functionals prefer the wurtzite type for the lithium halogenides instead of the rock-salt type

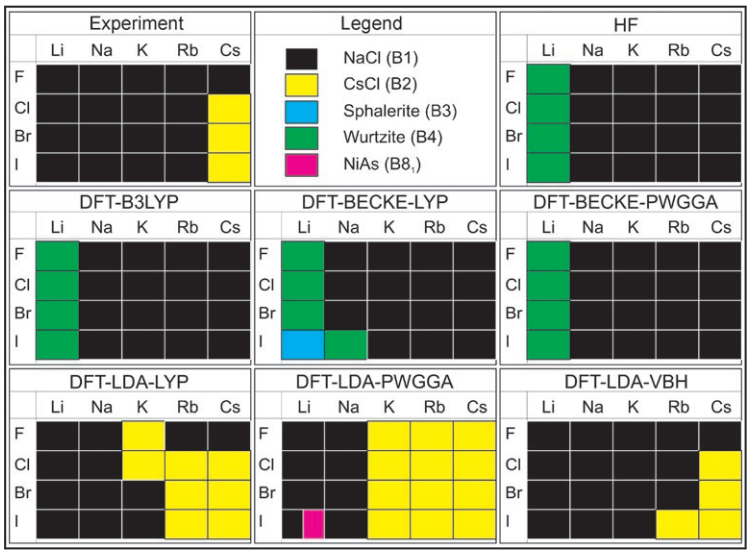

Figure 2. Overview of the seven ab initio techniques (Hartree–Fock plus six different DFT approximations) for the 20 alkali metal halides. For each alkali metal halide, the modification that is calculated to be thermodynamically stable at standard pressure and zero temperature is indicated. Experiment refers to standard pressure and temperature.

and the rock-salt type instead of the CsCl type for CsCl, CsBr, and CsI, whereas LDA-LYP and LDA-PWGGA assign the CsCl type to most of the rubidium and potassium halogenides instead of the experimentally observed rock-salt type.

Stability Regions as a Function of Pressure

Figures 3–7 show the stability regions as a function of pressure in the form of one-dimensional phase diagrams for the 20 alkali metal halide systems investigated for intermediary positive and negative pressures in the general range of −10 to +10 GPa. The corresponding $E(V)$ curves and the crystallographic data of the optimized structures are given in the Supporting Information. Without going into much detail, we note the overall similarity of the sequence of modifications of a given system as a function of pressure for all seven ab initio methods. Some modifications appear only for very small pressure ranges as barely stable phases, and are sometimes even missing, depending on the ab initio method; however, the $E(V)$ curves clearly indicate that these phases have nearly the same enthalpy in these pressure ranges as the supposedly thermodynamically stable phase.

Moreover, there appear to be some systematic shifts of the transition pressures with the calculation method: usually, calculations with Hartree–Fock and Becke-type functionals result in the highest transition pressures (BECKE-LYP slightly ahead of the other three methods with BECKE-PWGGA trailing a bit behind), whereas LDA-VBH, LDA-PWGGA, and LDA-LYP, in this order, usually produce transition pressures several GPa lower than those computed with Hartree–Fock, with LDA-LYP being the most extreme case. This agrees to a large degree with the observations of the dependence of transition pressures on the ab initio method for the alkali metal sulfides.[13] Similarly, the pressure range over which intermediary phases are stable—such as those exhibiting the wurtzite or 5–5 structure type that lie between the β-BeO and the rock-salt phase, or the rock-salt phase located between the

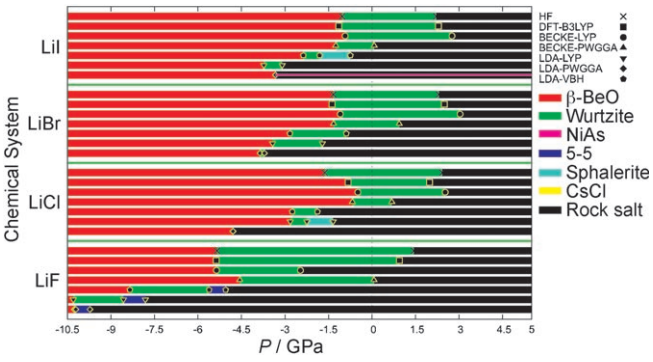

Figure 3. Low-temperature modifications of lithium halides, LiX, as a function of pressure (X = F, Cl, Br, I). The corresponding $E(V)$ curves for the LiX systems are given in the Supporting Information. As discussed, for example, in reference [15], for a given pressure several possible modifications usually exist that are only separated by a very small amount of enthalpy (compare the $E(V)$ curves for the LiX systems). Only the modifications with the lowest enthalpy are depicted for both the Hartree–Fock (HF) and the six different correlation-exchange functionals.

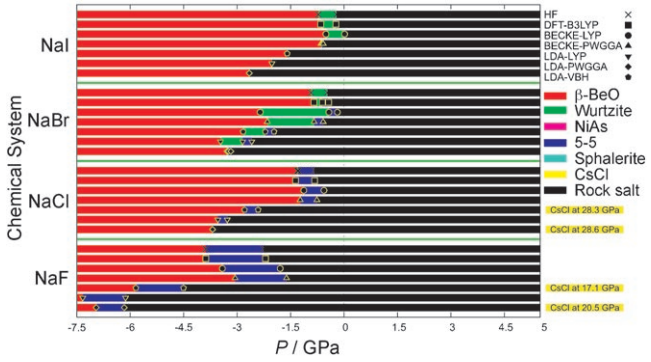

Figure 4. Low-temperature modifications of sodium halides, NaX, as a function of pressure (X = F, Cl, Br, I). The corresponding $E(V)$ curves for the NaX systems are given in the Supporting Information. As discussed, for example, in reference [15], for a given pressure several possible modifications usually exist that are only separated by a very small amount of enthalpy (compare the $E(V)$ curves for the NaX systems). Only the modifications with the lowest enthalpy are depicted for both the Hartree–Fock (HF) and the six different correlation-exchange functionals. For details, see Figure 3.

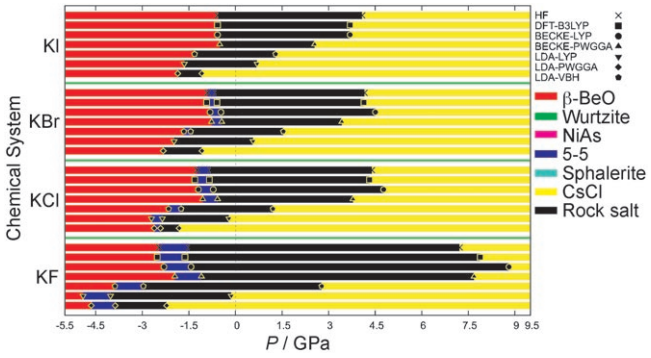

Figure 5. Low-temperature modifications of potassium halides, KX, as a function of pressure (X = F, Cl, Br, I). The corresponding $E(V)$ curves for the KX systems are given in the Supporting Information. As discussed, for example, in reference [15], for a given pressure several possible modifications usually exist that are only separated by a very small amount of enthalpy (compare the $E(V)$ curves for the KX systems). Only the modifications with the lowest enthalpy are depicted for both the Hartree–Fock (HF) and the six different correlation-exchange functionals. For details see Figure 3.

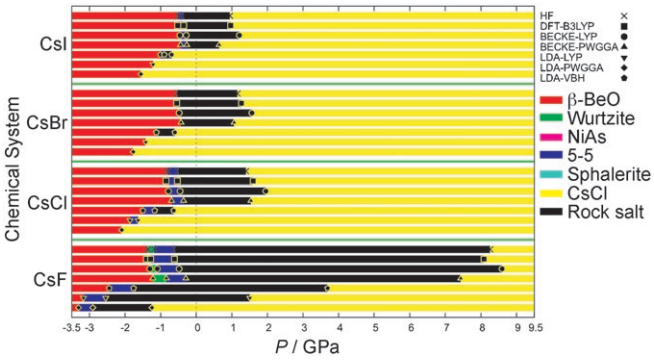

Figure 7. Low-temperature modifications of cesium halides, CsX, as a function of pressure (X = F, Cl, Br, I). The corresponding $E(V)$ curves for the CsX systems are given in the Supporting Information. As discussed, for example, in reference [15], for a given pressure several possible modifications usually exist that are only separated by a very small amount of enthalpy (compare the $E(V)$ curves for the CsX systems). Only the modifications with the lowest enthalpy are depicted for both the Hartree–Fock (HF) and the six different correlation-exchange functionals. For details see Figure 3.

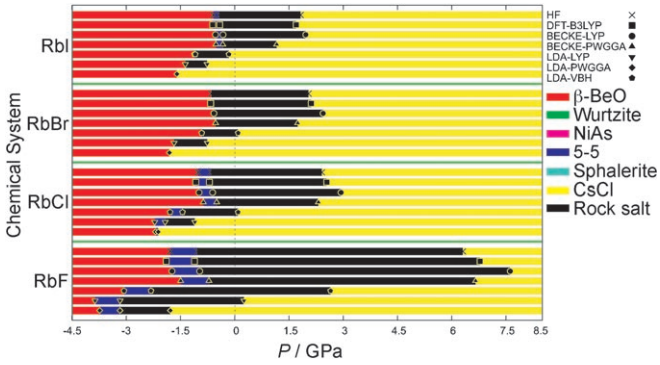

Figure 6. Low-temperature modifications of rubidium halides, RbX, as a function of pressure (X = F, Cl, Br, I). The corresponding $E(V)$ curves for the RbX systems are given in the Supporting Information. As discussed, for example, in reference [15], for a given pressure several possible modifications usually exist that are only separated by a very small amount of enthalpy (compare the $E(V)$ curves for the RbX systems). Only the modifications with the lowest enthalpy are depicted for both the Hartree–Fock (HF) and the six different correlation-exchange functionals. For details see Figure 3.

particular low-density modification stable at slightly negative presssures (β-BeO, wurtzite, or 5–5 structure type) and the CsCl type—is largest for the Hartree–Fock and Becke-type functionals and strongly decreases in size over LDA-VBH and LDA-PWGGA to LDA-LYP. Besides these interesting but not unexpected trends, this comparison suggests that the accuracy of the calculated transition pressures is limited to several GPa.

Taking the general limitations of the accuracy of the ab initio calculations into account, we found satisfactory agreement between observed and calculated phases as a function of pressure. We recall from Figure 2 that the method that yields the best overall agreement with experiment at standard pressure (without special adjustments of the basis set, etc., to fit experiments) for the alkali metal halides appears to be DFT with functional LDA-VBH.

Table 3 shows the calculated transition pressures for the B1→B2 transition for all the alkali metal halides computed at the Hartree–Fock and LDA-VBH levels, together with the experimental data. We can again see the trend that Hartree–Fock calculations show a higher transition pressure than LDA-based ones. On the other hand, it appears as if the pressure–homologue rules are not always obeyed. However, when the size of the pressure range of the intermediary phases is considered as a function of anion size for a fixed cation, this size decreases with increasing anion radius and is essentially independent of the ab initio method employed. Similarly, for a given anion, the size of the range of the intermediary phases decreases with increasing cation radius. Thus, we would suggest that the pressure–homologue rule may be only part of a larger rule, which states that in homologue families of binary (ionic) compounds, the pressure range over which intermediary structure types are stable modifications decreases with increasing cation or anion size for a fixed anion or cation, respectively.

Discussion

As mentioned in the previous section, we observed the usual systematic over- and underestimation of various physical quantities such as lattice parameters, transition pressures, and bulk moduli, which are typical of the various ab initio methods. For the alkali metal halides, the effects can be particularly large in the case of Hartree–Fock calculations: With regard to the lattice parameters, the errors increased systematically with increasing size of the cation and anion. The reason for this difference is the much higher relative importance of dispersion and polarization for larger atoms. Generally, the $E(V)$ curves of the alkali metal halides are

Table 3. Transition pressures (GPa) for the B1→B2 transition in the alkali metal halides.[a]

	Method	F	Cl	Br	I
Li	LDA-VBH	./.	./.	./.	./.
	HF	./.	./.	./.	./.
	Experiment	./.[101]	./.[101]	./.[101]	./.[101]
	Theory	252[106]	79–185[104–106]	94[106]	112[106]
Na	LDA-VBH	+17.1	+28.3	+70	./.
	HF	+32.0	+30.0	./.	./.
	Experiment	27–29[92,101,102]	28–30[92,100–102]	B1→CrB (HP)[92,93,102]	B1→CrB (HP)[92,93,102]
	Theory	12.1–32.6[103,105,106]	21.2–38.3[103–106]	15.9–19.1[103,106]	15.5–21.1[103,106]
K	LDA-VBH	+2.8	+1.0	+1.5	+1.5
	HF	+7.3	+4.6	+4.3	+4.3
	Experiment	1.7–4.0[99,101]	1.97[99,101]	1.81[99,101]	1.79[99,101]
	Theory	5.6[106]	2.0–4.5[104–106]	1.6[106]	2.7[106]
Rb	LDA-VBH	+0.3	+0.2	+0.1	−0.1
	HF	+6.2	+2.7	+2.0	+1.7
	Experiment	0.9–3.5[99,101]	0.49[99,101]	0.45[99,101]	0.40[99,101]
	Theory	−0.8[106]	0.1–0.2[104,106]	0.0–2.5[105,106]	0.8[106]
Cs	LDA-VBH	+3.7	−0.5	−0.5	−0.8
	HF	+8.2	+1.5	+1.2	+1.0
	Experiment	(2.0)[99,101]	./.	./.	./.
	Theory	−4.9[106]	−1.8[106]	−1.8[106]	−0.9[106]

[a] Computed by DFT with the LDA-VBH functional and the Hartree–Fock approximation, together with the experimental data and some theoretical results. Only transition pressures below 100 GPa are listed for the present calculations. In the case of NaBr and NaI, the actual transition goes from the B1 type to a distorted-B1 structure and the TlI (CrB-HP/GeS) structure type (B16) in the range 33–40 and 27–32 GPa, respectively.[92,93] CsCl, CsBr, and CsI exhibit tetragonal, and subsequently perhaps orthorhombic, distortions from the B2 structure under high pressure (probably around 65, 53, and 35 GPa, respectively).[94–98] The theoretical data include ab initio level calculations and calculations with refined empirical potentials. The symbol ./. indicates that up to 100 GPa, no B1→B2 transition was found in experiment or the theoretical calculations in this work. The value in brackets indicates that the experimental transition pressure is only a rough estimate.

very flat and the bulk moduli are relatively small, because the bulk modulus is evaluated from the second derivative of the energy at the calculated equilibrium geometry (at the minimum). Here, when small ions and larger electrostatic forces are involved, as in the case of the oxides,[15] sulfides,[45,13] and nitrides,[6] the calculated bulk moduli are closer to the experimental values than for the alkali metal halides. The systematic comparison of experiment with density-functional-based calculations is not quite as straightforward owing to the large number of different functionals employed. Nevertheless, one finds again systematic trends that agree with those typically observed, especially for the functionals based on the local density approximation. Naturally, the cation–anion nearest-neighbor distances in the extended solid are longer (by 15–25%) than those found in calculations and experiment for the monomers MX in the gas phase.[107,108]

In general, our calculations fit quite well with computations of the alkali metal halides found in the literature (Table 2). Furthermore, the systematic trends in the values of the physical parameters as a function of the ab initio method are essentially the same as those we found for the alkali metal sulfides, for which we also compared a large number of ab initio methods.[13]

As discussed in the previous section, analysis of the one-dimensional pressure–phase diagrams suggests that the focus should actually be less on the sequence of transition pressures and more on the size of the stability ranges of the individual modifications as a function of cation/anion size. This agrees well with our observations for the alkali metal sulfides[13] and oxides,[15] and for the alkaline earth oxides,[14] for which the size of the stability range of intermediary modifications also decreased with increasing cation size for fixed anions within a family of compounds. In this context, one should stress the fact that there are usually many different modifications that are in close competition for thermodynamic stability at a given pressure; for example, the $E(V)$ curves indicate that the NiAs type should be a good candidate at high pressures for the lithium halides. Furthermore, one often finds slightly distorted variants of the thermodynamically stable modification that might be stable within some limited range of pressures before a transition to a substantially different structure type occurs—examples are the high-pressure phases of the cesium halides found in experiment, or the orthorhombically distorted Ni_2In structure found in the calculation of high-pressure modifications of the alkali metal sulfides.[13] Clearly, these distortions can be explored to a certain degree with ab initio calculations. However, when performing structure prediction in not-yet-explored systems, one usually hesitates to focus on these minor variations on a theme because the energy differences between the distorted and undistorted structures are often smaller than the estimated errors of the ab initio energy calculations themselves. In this context, we did not include ab initio calculations of the high-pressure phases of NaBr and NaI, and similarly those of CsCl, CsBr, and CsI, in this study, as a comparison of their transitions with the B1–B2 transitions present in the other alkali metal halides would not have been useful within the context of this investigation.

Finally, we found that in most alkali metal halides, the first metastable phase that becomes thermodynamically stable at negative pressures is the so-called 5–5 structure consisting of trigonal bipyramids of A anions about B cations, which can be visualized as an ionic structural analogue to the hexagonal boron nitride structure. This structure was first discovered over a decade ago by using global explorations on the energy landscape of the NaCl system;[36] more recently, it was found on the landscapes of the alkaline earth oxides[14] and observed as a transition state in simulations of the wurtzite-to-rocksalt transition in ZnO.[109][11] Experimentally, this structure type was subsequently observed

[11] In this work, the 5–5 structure type was called the "hexagonal MgO" type.

to represent the binary aristotype of the ternary compound Li_4SeO_5,[110] in which Li and Se atoms occupy the cationic positions and O atoms the anionic positions in the 5–5 structure. Clearly, this structure type is a viable one from both experimental and theoretical points of view. It should definitely be possible to synthesize one of the alkali halides in this modification, perhaps by steering the reaction through an appropriate choice of substrate during a deposition from the gas phase, as was recently suggested for the deposition of NaBr on an $LiNbO_3$ substrate.[111]

Conclusions

We have investigated the enthalpy landscapes of the 20 binary alkali metal halide systems by using global optimization techniques to identify possible modifications of the alkali metal halides as a function of pressure and type of alkali metal and halogen. Both Hartree–Fock and density functional calculations (for six different functionals) were performed to refine the candidate structures and to compute the pressure ranges over which these modifications are thermodynamically stable. The results are in good agreement with experiment, and we predict that in most of these systems the so-called 5–5 modification should be metastable at standard pressure and be thermodynamically stable at slightly negative pressures. The sizes of the pressure ranges over which the various modifications are stable show characteristic trends as a function of the type of constituent element, thus generalizing the traditional pressure–homologue rule for transition pressures and stable phases in ionic solids. Furthermore, the trends in the computed quantities such as transition pressures and lattice parameters as a function of the ab initio method are similar to those found in earlier theoretical studies of the alkali metal sulfides.

Acknowledgements

This work was supported by the BMBF through grant no. 03C0352.

[1] L. Liu, W. A. Bassett, *Elements, Oxides and Silicates: High-Pressure Phases with Implications for the Earth's Interior*, Oxford University Press, New York, **1986**.
[2] *Reviews in Mineralogy, Vol. 37: Ultrahigh-Pressure Mineralogy: Physics and Chemistry of the Earth's Deep Interior* (Ed.: R. J. Hemley), The Mineralogical Society of America, Washington, **1998**.
[3] D. Fischer, M. Jansen, *Angew. Chem.* **2002**, *114*, 1831–1833; *Angew. Chem. Int. Ed.* **2002**, *41*, 1755–1756.
[4] D. Fischer, M. Jansen, *J. Am. Chem. Soc.* **2002**, *124*, 3488.
[5] D. Fischer, M. Jansen, *Z. Anorg. Allg. Chem.* **2003**, *629*, 1934.
[6] D. Fischer, Ž. Čančarević, J. C. Schön, M. Jansen, *Z. Anorg. Allg. Chem.* **2004**, *630*, 156–160.
[7] J. C. Schön, M. Jansen, *Angew. Chem.* **1996**, *108*, 1358–1377; *Angew. Chem. Int. Ed. Engl.* **1996**, *35*, 1286–1304.
[8] S. M. Woodley, P. D. Battle, J. D. Gale, C. R. A. Catlow, *Phys. Chem. Chem. Phys.* **1999**, *1*, 2535–2542.
[9] C. Mellot Draznieks, J. M. Newsam, A. M. Gorman, C. M. Freeman, G. Ferey, *Angew. Chem.* **2000**, *112*, 2358–2363; *Angew. Chem. Int. Ed.* **2000**, *39*, 2270–2275.
[10] J. C. Schön, M. Jansen, *Z. Kristallogr.* **2001**, *216*, 307–325; J. C. Schön, M. Jansen, *Z. Kristallogr.* **2001**, *216*, 361–383.
[11] M. Jansen, *Angew. Chem.* **2002**, *114*, 3896–3917; *Angew. Chem. Int. Ed.* **2002**, *41*, 3746–3766.
[12] J. C. Schön, M. A. C. Wevers, M. Jansen, *J. Mater. Chem.* **2001**, *11*, 69–77.
[13] J. C. Schön, Ž. Čančarević, M. Jansen, *J. Chem. Phys.* **2004**, *121*, 2289–2304.
[14] J. C. Schön, *Z. Anorg. Allg. Chem.* **2004**, *630*, 2354–2366.
[15] Z. Cancarevic, J. C. Schön, M. Jansen, *Phys. Rev. B* **2006**, *73*, 224114.
[16] A. Neuhaus, *Chimia* **1964**, *18*, 93.
[17] E. Madelung. *Phys. Z* **1918**, *19*, 524.
[18] P. P. Ewald, *Ann. Phys.* **1921**, *64*, 253.
[19] M. Born, K. Huang, *Dynamical Theory of Crystal Lattices*, Oxford University Press, London, **1954**.
[20] B. G. Dick, A. W. Overhauser, *Phys. Rev.* **1958**, *112*, 90.
[21] K. Fischer, H. Blitz, R. Habernkorn, W. Weber, *Phys. Status Solidi B* **1972**, *54*, 285.
[22] U. Schröder, *Solid State Commun.* **1966**, *4*, 347.
[23] R. G. Gordon, Y. S. Kim, *J. Chem. Phys.* **1972**, *56*, 3122.
[24] A. J. Cohen, R. G. Gordon, *Phys. Rev. B* **1976**, *14*, 4593–4605.
[25] C. Muhlhauser, R. Gordon, *Phys. Rev. B* **1981**, *23*, 900.
[26] P. O. Löwdin, *Adv. Phys.* **1956**, *5*, 1.
[27] J. S. Malvin, D. C. Hendry, *J. Phys. C* **1982**, *15*, 2093.
[28] K. S. Chang, M. L. Cohen, *Phys. Rev. B* **1984**, *30*, 4774.
[29] J. Chen, L. L. Boyer, H. Krakauer, M. J. Mehl, *Phys. Rev. B* **1988**, *37*, 3295.
[30] P. Cortona, *Phys. Rev. B* **1992**, *46*, 2008–2014.
[31] P. Cortona, *Nuovo Cimento Soc. Ital. Fis. D* **1993**, *15*, 243.
[32] M. Causa, R. Dovesi, C. Pisani, C. Roetti, *Phys. Rev. B* **1986**, *33*, 1308.
[33] C. Pisani, R. Dovesi, C. Roetti, *Hartree–Fock Ab Initio Treatment of Crystalline Solids*, *Lecture Notes in Chemistry*, *Vol. 48*, Springer, Berlin, **1988**.
[34] M. Prencipe, A. Zupan, R. Dovesi, E. Apra, V. R. Saunders, *Phys. Rev. B* **1995**, *51*, 3391–3396.
[35] S. W. de Leeuw, J. W. Perram, E. R. Smith, *Proc. R. Soc. London Ser. A* **1980**, *373*, 27–56; S. W. de Leeuw, J. W. Perram, E. R. Smith, *Proc. R. Soc. London Ser. A* **1980**, *373*, 57–66,.
[36] J. C. Schön, M. Jansen, *Comput. Mater. Sci.* **1995**, *4*, 43–58.
[37] S. Kirkpatrick, C. D. Gelatt, Jr., M. P. Vecchi, *Science* **1983**, *220*, 671–680.
[38] V. Czerny, *J. Optim. Theo. Appl.* **1985**, *45*, 41–51.
[39] N. Metropolis, A. W. Rosenbluth, M. N. Rosenbluth, A. H. Teller, E. Teller, *J. Chem. Phys.* **1953**, *21*, 1087–1092.
[40] R. Hundt, J. C. Schön, A. Hannemann, M. Jansen, *J. Appl. Crystallogr.* **1999**, *32*, 413–416.
[41] A. Hannemann, R. Hundt, J. C. Schön, M. Jansen, *J. Appl. Crystallogr.* **1998**, *31*, 922–928.
[42] R. Hundt, J. C. Schön, M. Jansen, *J. Appl. Crystallogr.* **2006**, *39*, 6–16.
[43] R. Hundt, KPLOT: A Program for Plotting and Investigation of Crystal Structures, University of Bonn, Bonn (Germany), **1979**.
[44] V. R. Saunders, R. Dovesi, C. Roetti, M. Causa, N. M. Harrison, R. Orlando, C. M. Zicovich-Wilson, CRYSTAL2003, University of Torino, Torino (Italy), **2003**.
[45] Ž. Čančarević, J. C. Schön, M. Jansen, *Mater. Sci. Forum* **2004**, *453*, 71–76.
[46] F. D. Murnaghan, *Proc. Natl. Acad. Sci. USA* **1944**, *30*, 244–247.
[47] "CRYSTAL Basis Sets Library", to be found under http://www.crystal.unito.it/Basis_Sets/Ptable.html, **2006**.
[48] http://www.theochem.uni-stuttgart.de/, **2006**.
[49] M. A. C. Wevers, J. C. Schön, M. Jansen, *J. Solid State Chem.* **1998**, *136*, 223–246.

[50] K. Doll, J. C. Schön, M. Jansen, *Phys. Chem. Chem. Phys.* **2007**, *9*, 6128–6133.
[51] J. C. Schön, H. Putz, M. Jansen, *J. Phys. Condens. Matter* **1996**, *8*, 143–156.
[52] M. Prencipe, PhD thesis, University of Torino (Italy), **1990**.
[53] "Total energy and related properties": R. Dovesi in *Quantum-Mechanical Ab-initio Calculation of the Properties of Crystalline Materials*, *Lecture Notes in Chemistry*, *Vol. 67* (Ed.: C. Pisani), Springer, Berlin, **1996**.
[54] P. Debye, P. Scherrer, *Phys. Z.* **1916**, *17*, 277–283.
[55] A. W. Hull, *Trans. Am. Inst. Electr. Eng.* **1919**, *38*, 1445–1466.
[56] H. Ott, *Z. Krist. Kristallgeom. Kristallphys. Kristallchem.* **1926**, *63*, 222–230.
[57] G. J. Finch, S. Fordham, *Proc. Phys. Soc. London* **1936**, *48*, 85–94.
[58] J. Thewlis, *Acta Crystallogr.* **1955**, *8*, 36–38.
[59] V. A. Streltsov, V. G. Tsirelson, R. P. Ozerov, O. A. Golovanov, *Kristallografiya* **1988**, *33*, 90–97.
[60] K. Recker, F. Wallrafen, K. Dupre, *Naturwissenschaften* **1988**, *75*, 156–157.
[61] R. F. S. Hearmon in *Elastic, Piesoelectric and Related Constants of Crystals*, *Landolt-Boernstein, Group III*, *Vol. 11* (Eds.: K. H. Hellwege, A. M. Hellwege), Springer, New York, **1979**.
[62] E. Posnjak, R. W. G. Wyckoff, *J. Wash. Acad. Sci.* **1922**, *12*, 248–251.
[63] H. Ott, *Phys. Z.* **1923**, *24*, 209–213.
[64] A. F. Levinsh, M. E. Straumanis, K. Karlsons, *Z. Phys. Chem. Abt. B* **1938**, *40*, 146–150.
[65] P. Debye, P. Scherrer, *Phys. Z.* **1918**, *19*, 474–483.
[66] W. L. Bragg, *Nature* **1920**, *105*, 646–648.
[67] T. Barth, G. Lunde, *Zentralblatt Miner. Geol. A* **1927**, *1927*, 57–66.
[68] V. P. Deshpande, *Acta Crystallogr.* **1961**, *14*, 794–794.
[69] R. B. Srinivasa, S. P. Sanyal, *Phys. Rev. B* **1990**, *42*, 1810–1816.
[70] W. H. Bragg, W. L. Bragg, *Proc. R. Soc. London Ser. A* **1913**, *88*, 428–428.
[71] M. E. Straumanis, A. Jevins, *Z. Phys.* **1936**, *102*, 353–359.
[72] J. E. Nickels, M. A. Fineman, W. E. Wallace, *J. Phys. Chem.* **1949**, *53*, 625–628.
[73] W. T. Barrett, W. E. Wallace, *J. Am. Chem. Soc.* **1954**, *76*, 366–369.
[74] S. C. Abrahams, J. L. Bernstein, *Acta Crystallogr.* **1965**, *18*, 926–932.
[75] V. S. Urusov, V. V. Blinov, *Izv. Akad. Nauk SSSR Ser. Khim.* **1970**, *12*, 278–282.
[76] L. W. Finger, H. King, *Am. Mineral.* **1978**, *63*, 337–342.
[77] H. E. Swanson, W. P. Davey, *Nat. Bur. Stand. Circular* **1955**, *539*, 31–32.
[78] H. E. Swanson, M. Mehmel, *Nat. Bur. Stand. Circular* **1955**, *539*, 31–32.
[79] H. E. Swanson, E. Posnjak, R. W. G. Wyckoff, *Nat. Bur. Stand. Circular* **1955**, *539*, 31–32.
[80] E. Broch, I. Oftedal, A. Pabst, *Z. Phys. Chem. Abt. B* **1929**, *3*, 209–214.
[81] E. Wagner, *Ann. Phys.* **1916**, *49*, 625–647.
[82] M. Ahtee, *Ann. Acad. Sci. Fenn. Ser. A1* **1969**, *313*, 1–11.
[83] L. Vegard, *Z. Phys.* **1921**, *5*, 17–26.
[84] V. M. Goldschmidt, *Skr. Nor. Vidensk.-Akad. Kl. 1* **1926**, 1.
[85] S. von Ohlshausen, *Z. Krist. Kristallgeom. Kristallphys. Kristallchem.* **1925**, *61*, 463–514.
[86] L. H. Adams, B. L. Davis, *Proc. Natl. Acad. Sci. USA* **1962**, *48*, 982–990.
[87] "The coherent neutron scattering amplitude of Rb: A neutron diffraction study of RbCl": F. F. Y. Wang, *Acta Crystallogr. Sect. A* **1970**, *26*, 377–379.
[88] W. P. Davey, *Phys. Rev.* **1921**, *17*, 402–403.
[89] W. P. Davey, *Phys. Rev.* **1922**, *19*, 538–538.
[90] C. D. West, *Z. Krist. Kristallgeom. Kristallphys. Kristallchem.* **1934**, *88*, 94–94.
[91] M. Blackman, I. H. Khan, *Proc. Phys. Soc. London* **1961**, *77*, 471–475.
[92] Y. Sato-Sorensen, *J. Geophys. Res.* **1983**, *88*, 3543.
[93] J. M. Leger, J. Haines, A. Atouf, *Phys. Rev. B* **1998**, *51*, 3902.
[94] T.-L. Huang, A. L. Ruoff, *Phys. Rev. B* **1984**, *29*, 1112.
[95] E. Knittle, R. Jeanloz, *Science* **1984**, *223*, 53.
[96] Y. K. Vohra, K. E. Brister, S. T. Weir, S. J. Duclos, A. L. Ruoff, *Science* **1986**, *231*, 1136.
[97] E. Knittle, R. Jeanloz, *J. Phys. Chem. Solids* **1985**, *46*, 1179.
[98] E. Knittle, A. Rudy, R. Jeanloz, *Phys. Rev. B* **1985**, *31*, 588.
[99] P. W. Bridgman, *Proc. Am. Acad. Arts Sci.* **1945**, *76*, 1.
[100] X. Li, R. Jeanloz, *Phys. Rev. B* **1987**, *36*, 474.
[101] C. W. F. T. Pistorius, *Prog. Solid State Chem.* **1976**, *11*, 1.
[102] S. J. Duclos, Y. K. Vohra, A. L. Ruoff, S. Filipek, B. Baranowski, *Phys. Rev. B* **1987**, *36*, 7664.
[103] B. S. Rao, S. P. Sanyal, *Phys. Rev. B* **1990**, *42*, 1810.
[104] A. M. Pendas, V. Luana, J. M. Recio, M. Florez, E. Francisco, M. A. Blanco, L. N. Kantorovich, *Phys. Rev. B* **1994**, *49*, 3066.
[105] C. E. Sims, G. D. Barrera, N. L. Allan, W. C. Mackrodt, *Phys. Rev. B* **1998**, *57*, 11164.
[106] M. Florez, J. M. Recio, E. Francisco, M. A. Blanco, A. M. Pendas, *Phys. Rev. B* **2002**, *66*, 144112.
[107] A. C. Olleta, H. M. Lee, K. S. Kim, *J. Chem. Phys.* **2006**, *124*, 024321.
[108] A. C. Olleta, H. M. Lee, K. S. Kim, *J. Chem. Phys.* **2007**, *126*, 144311.
[109] S. Limpijumnong, W. R. L. Lambrecht, *Phys. Rev. B* **2001**, *63*, 104103.
[110] H. Haas, M. Jansen, *Angew. Chem.* **1999**, *111*, 2033–2035; *Angew. Chem. Int. Ed.* **1999**, *38*, 1909–1911.
[111] J. C. Schön, T. Dinges, M. Jansen, *Z. Naturforsch. B* **2006**, *61*, 650–659.

Received: September 26, 2007
Published online: February 19, 2008

